Implementation of a Hyperchaotic System with Hidden Attractors into a Microcontroller

Angelos E. Giakoumis, Christos K. Volos[a], Ioannis N. Stouboulos, Ioannis K. Kyprianidis

Department of Physics, Aristotle University of Thessaloniki, GR-54124, Greece

Abstract. In this work, the implementation of a hyperchaotic oscillator by using a microcontroller is proposed. The dynamical system, which is used, belongs to the recently new proposed category of dynamical systems with hidden attractors. By programming the microcontroller, the three most useful tools of nonlinear theory, the phase portrait, the Poincaré map and the bifurcation diagram can be produced. The comparison of these with the respective simulation results, which are produced by solving the continuous dynamical system with Runge-Kutta, verified the feasibility of the proposed method. The algorithms could be easily modified to add or substitute the hyperchaotic system.

1 Introduction

In the last decades, nonlinear systems and especially chaotic systems have aroused tremendous interest because of their applications in many scientific fields, such as in social sciences, ecology, electronic circuits, lasers, chemical reactions, fluid dynamics, mechanical systems, etc. [1, 2], but also of many other interesting applications such as in secure communication schemes, cryptography and robotics [3-5].

At the same period, there has been an exponential use of embedded systems due to the advances in technology, new communication networks and cost-effective solutions. In general, an embedded system is a computer system used for a specific application such as a washing machine, robotics, automotive, television, cameras, etc. [6-8]. It is basically a compound of a microprocessor, memory and peripherals. In recent years, there are several embedded applications based on microcontroller such as in military, industry, banking transference, e-commerce, biometric systems, cryptography, robotics, telemedicine, and computing [6], [9-18].

Literature presents in the last few years some advances of implementing chaotic systems and their applications with a microcontroller. In 2012, two works based on a microcontroller have been presented, in which the authors presented a simple implementation of the logistic map [19, 20]. Each one of the above papers presents the implementation of a chaotic cryptosystem. The same year, Stanciu and Datcu presented an Atmel AVR microcontroller implementation of a new encryption algorithm based on chaos [21]. In 2013, Volos *et al*. investigated experimentally the coverage performance of a chaotic autonomous mobile robot for fast scanning of the robots workspace with unpredictable way, in which each one of the two robot's independent active wheels is driven by two chaotic logistic maps implemented with Arduino Uno microcontroller [22]. In the same year, Chiu *et al*. proposed an experimental implementation in a microcontroller of the chaotic Lorenz system in order to demonstrate that this kind of chaotic oscillator can be achieved in a digital system like this [23]. Also, in 2013, Volos presented a microcontroller implementation of a chaotic random bit generator with very good statistical results [24].

In 2014, Ketthong and San-Um presented a new random-bit generator based on a new signum-based piecewise-linear chaotic map [25]. Also, in 2014, the same authors proposed a generalization of four chaotic maps with absolute value nonlinearity [26], which is experimentally implemented by using an Arduino microcontroller. Furthermore, Andreatos and Volos in 2014 presented a microcontroller implementation of a text encryption algorithm based on a chaotic Chua system [27]. In 2015, Zapateiro *et al*. [28] presented an experimental realization of a chaos-based secure communication by using Arduino microcontroller.

In this paper, the implementation of a hyperchaotic oscillator with hidden attractors, by using a microcontroller, is proposed. Hidden attractors cannot be localized by using the standard computational procedure; therefore it is difficult to predict the existence of them in a considered system [29, 30]. Furthermore, there has been a significant interest in studying hidden attractors because they play an important role both in theoretical problems and practical engineering applications [31, 32]. Hidden attractors appear in numerous dynamical systems such as Chua's circuit [33], van der Pol–Duffing oscillators [34], model of drilling system actuated by induction motor [35], Lorenz–like system describing convective fluid motion [36], or multilevel DC/DC converter [37].

[a] Corresponding author: volos@physics.auth.gr

This paper is organized as follows. In Section 2 the proposed hyperchaotic system with hidden attractors is analyzed. Section 3 presents the realization of the system with the microcontroller as well as the phase portraits, the Poincaré maps and the bifurcation diagram, which are obtained from the microcontroller. Finally, the conclusions are drawn in Section 4.

2 The Proposed System

In this work, the simplest four-dimensional hyperchaotic Lorenz-type system, which has been proposed by Gao and Zhang [38], is used. This system is an extension of a modified Lorenz system, which was studied by Schrier and Maas as well as by Munmuangsaen and Srisuchinwong [39, 40]. The proposed system is described by the following set of differential equations.

$$\begin{cases} \dot{x} = y - x \\ \dot{y} = -xz + u \\ \dot{z} = xy - a \\ \dot{u} = -by \end{cases} \quad (1)$$

It is structurally a very simple four-dimensional dynamical system having only two independent parameters (a, b). Also, it has many interesting properties not found in other proposed systems, such as:

- It has very few terms, only seven with two quadratic nonlinearities, and two parameters.
- All its attractors are hidden.
- It exhibits hyperchaos over a large region of parameter space.
- Its Jacobian matrix has rank less than four everywhere in the space of the parameters.
- It exhibits a quasiperiodic route to chaos with an attracting torus for some choice of parameters.
- It has regions in which the torus coexists with either a symmetric pair of strange attractors or a symmetric pair of limit cycles and other regions where three limit cycles coexist.
- The basins of attraction have an intricate fractal structure.
- There is a series of Arnold tongues [41] within the quasi-periodic region where the two fundamental oscillations mode-lock and form limit cycles of various periodicities.

In this Section the system's dynamic behavior is investigated numerically by employing a fourth order Runge-Kutta algorithm. For this reason, the bifurcation diagram, which is a very useful tool from nonlinear theory, is used. In Figure 1(a) the bifurcation diagram of the variable y versus the parameter b, for $a = 2.5$, reveals the richness of system's dynamical behavior. Besides limit cycles, the system (1) has quasiperiodicity, chaos, and hyperchaos.

Figure 1(b) shows the Lyapunov exponents' spectra, which is produced by using the Wolf's algorithm [42] for the chosen value of the parameter a ($a = 2.5$). As we can see, when the system has a periodic behavior all the Lyapunov exponents are $L_i \leq 0$ (i = 1, 2, 3, 4), while when it has chaotic or hyperchaotic behavior the system appears one or two positive Lyapunov exponents. So, from Fig. 1(b) the system's hyperchaotic behavior is found for example in the range of $b \in [0.313, 0.462]$, where the system has two positive Lyapunov exponents, as it is shown in the embedded diagram in Fig. 1(b).

In more details, as a value of a decreased from $a = 0.9$ the system goes from a period-1 steady state, through a quasi-periodic route, to the chaotic state. The limit cycle of period-1 and the quasiperiodic attractor in (y, z)-plane are shown in Fig. 6(a) and Fig. 7(a) for $b = 0.9$ and $b = 0.8$, respectively. Also, the chaotic behavior of the proposed system is confirmed by the attractor in (y, z)-plane, for $b = 0.55$, which is shown in Fig. 8(a). However, a very interesting feature of the specific system is the existence of hyperchaotic attractor for the range of parameter b, which is mentioned before, as it is shown in the phase portraits of Fig. 9(a).

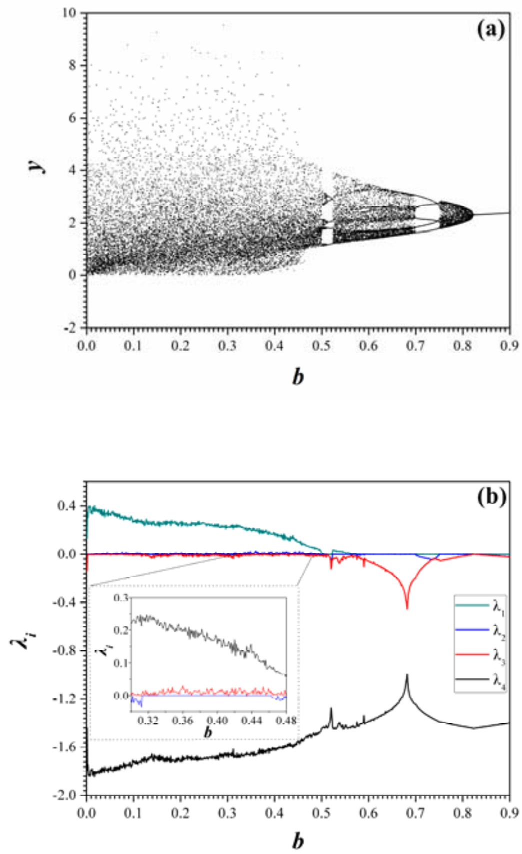

Figure 1. (a) Bifurcation diagram of y versus b, and (b) the diagram of Lyapunov exponents (λ_i) versus the parameter b, for $a = 2.5$.

3 Experimental Results

In this work, we use the PIC32MX795F512H 32-bits microcontroller from Microchip with up to 80 MHz of bus frequency on the Maximite board, which is a small and versatile computer board running MM Basic, a powerful Basic interpreter with floating point arithmetic and 128K working memory (Fg. 2). The data are stored in a .dat file in a 1MB SD card.

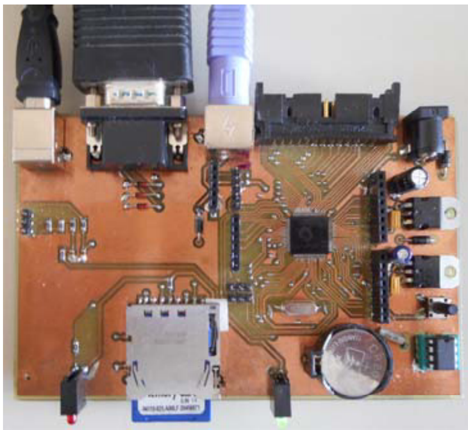

Figure 2. The PIC32MX795F512H 32-bits microcontroller from Microchip on the Maximite board.

In order to implement the oscillator with hidden attractors into the microprocessor, we use the four-dimensional hyperchaotic Lorenz-type system in discrete mode, using the Euler method [43]. So, the system takes the form

$$\begin{cases} X(k+1) = X(k) + h\left[Y(k) - X(k)\right] \\ Y(k+1) = Y(k) + h\left[-X(k)Z(k) + U(k)\right] \\ Z(k+1) = Z(k) + h\left[X(k)Y(k) - a\right] \\ U(k+1) = U(k) + h\left[-bY(k)\right] \end{cases} \tag{2}$$

Here $X(k)$, $Y(k)$, $Z(k)$ and $U(k)$ make up the system state, with the same parameters values, a, b, while h = 0.002 is the sampling time.

Next, the procedure with which the phase portrait, the Poincaré map and the bifurcation diagram produced, are described in details.

3.1 Phase Portrait

To test the implementation, the code shown in Fig. 3 was implemented using the MM Basic interpreter. Therefore, a file containing the $X(k)$, $Y(k)$, $Z(k)$ and $U(k)$ of system (2), which result to the variables $x(t)$, $y(t)$, $z(t)$ and $u(t)$ of the continuous dynamical system (1), is taken.

Figures 6(b), 7(b), 8(b) and 9(b) display the phase portraits in (Y, Z)-plane for a = 2.5 and for the same values of parameter b, as for the respective phase portraits in (y, z)-plane, which were produced by solving the system (1). From the comparison of the two series of phase portraits a very good agreement between them has been observed.

3.2 Poincaré Map

Next, the well-known Poincaré map, which is also a very useful tool in nonlinear theory, is used. This diagram is generated when system's trajectory intersects a selected plane in the phase space (X = 0) with $X(k + 1) > 0$. In this way, the program code shown in Fig. 4 was implemented using the MM Basic interpreter. So, from the microcontroller, a series of files containing the variables $Y(k)$, $Z(k)$ and $U(k)$, produced with the aforementioned procedure, for a = 2.5 and for various values of parameter b, are taken. From these files the Poincaré maps of Fig. 10, which confirm the expected dynamical behavior, are produced.

```
Rem  PROGRAM  BIFURCATION
xn1 = 0.2
yn1 = -0.1
zn1 = 0.3
wn = 0.1
c = 2.5
d = 0.9
h = 0.002
NTR = 200000
OPEN "php.DAT"  FOR  OUTPUT  AS #1
FOR I = 1 TO 1200000
xn = xn1
yn = yn1
zn = zn1
wn = wn1
xn1 = xn + h*(yn - xn)
yn1 = yn + h*(- xn*zn + wn)
zn1 = zn + h*(xn*yn - c)
wn1 = wn + h*(-d*yn)
IF  I > NTR  THEN  PRINT  #1, xn1, yn1, zn1, wn1
NEXT I
CLOSE #1
END
```

Figure 3. Program code used to extract the variables X, Y, Z, U for system's phase portrait with the microcontroller.

```
Rem  PROGRAM  POINCARE
xn1 = 0.2
yn1 = -0.1
zn1 = 0.3
wn = 0.1
c = 2.5
d = 0.8
h = 0.002
OPEN "poin.DAT"  FOR  OUTPUT   As #1
NTR = 200000
FOR  I = 1  TO  20000000
xn = xn1
yn = yn1
zn = zn1
wn = wn1
xn1 = xn + h*(yn - xn)
yn1 = yn + h*(- xn*zn + wn)
zn1 = zn + h*(xn*yn - c)
wn1 = wn + h*(-d*yn)
dy = 0.001
IF I > NTR THEN
IF xn > -dy And xn < dy  THEN
IF (yn - xn) > 0 THEN
PRINT  #1,  yn1, zn1, wn1
EndIf
EndIf
EndIf
NEXT I
CLOSE #1
END
```

Figure 4. Program code used to extract the variables Y, Z, U, for system's Poincaré map with the microcontroller.

3.3 Bifurcation Diagram

Finally, a third code shown in Fig. 5 was implemented using the MM Basic interpreter. With this code the microcontroller was programmed to generate a bifurcation diagram by extracting in a file the variables Y, Z and U versus the parameter b. The bifurcation diagram produced by obtained sequential Poincaré maps as the bifurcation parameter (b) decreased with step 0.001. In Fig. 11 the bifurcation diagram, which is produced by the capturing from the microcontroller data, is depicted. From the comparison of this diagram with the bifurcation diagram (Fig. 1(a)), which is produced by solving with Runge-Kutta the continuous system (1), a good agreement between them can be observed. However, a slightly different dynamical behavior can be observed in some small regions of parameter b, which occurred due to the different integrating methods.

```
Rem   PROGRAM   BIFURCATION
xn1 = 0.2
yn1 = -0.1
zn1 = 0.3
wn = 0.1
c = 2.5
d = 0.8
h = 0.002
OPEN "bif.DAT"   FOR  OUTPUT   As #1
DO
NTR = 200000
FOR  I = 1  TO  20000000
xn = xn1
yn = yn1
zn = zn1
wn = wn1
xn1 = xn + h*(yn - xn)
yn1 = yn + h*(- xn*zn + wn)
zn1 = zn + h*(xn*yn - c)
wn1 = wn + h*(-d*yn)
dy = 0.001
IF I > NTR THEN
IF xn > -dy And xn < dy  THEN
IF (yn - xn) > 0 THEN
PRINT  #1,  yn1, zn1, wn1
EndIf
EndIf
EndIf
NEXT I
IF d >= 0 THEN  d = d - 0.001
LOOP UNTIL d < 0
CLOSE #1
END
```

Figure 5. Program code used to extract the variables *Y*, *Z*, *U*, for system's bifurcation diagram with the microcontroller.

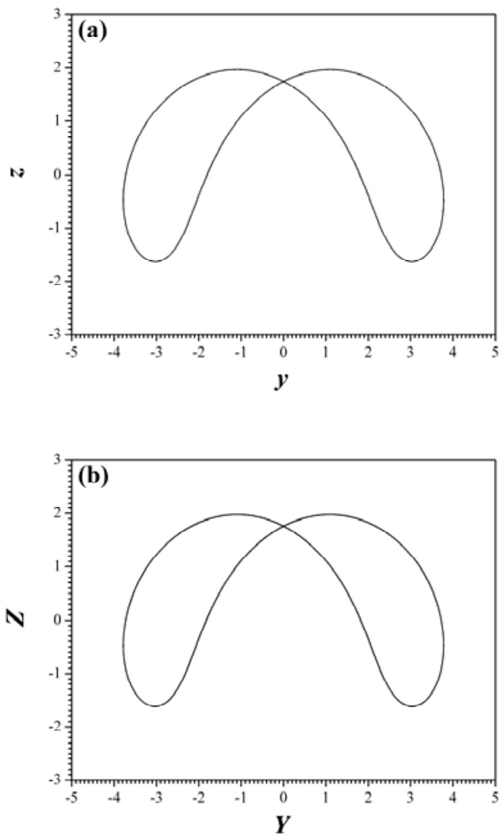

Figure 6. (a) Phase portrait of *z* versus *y* and (b) phase portrait of *Z* versus *Y*, for $a = 2.5$ and $b = 0.9$ (period-1 state).

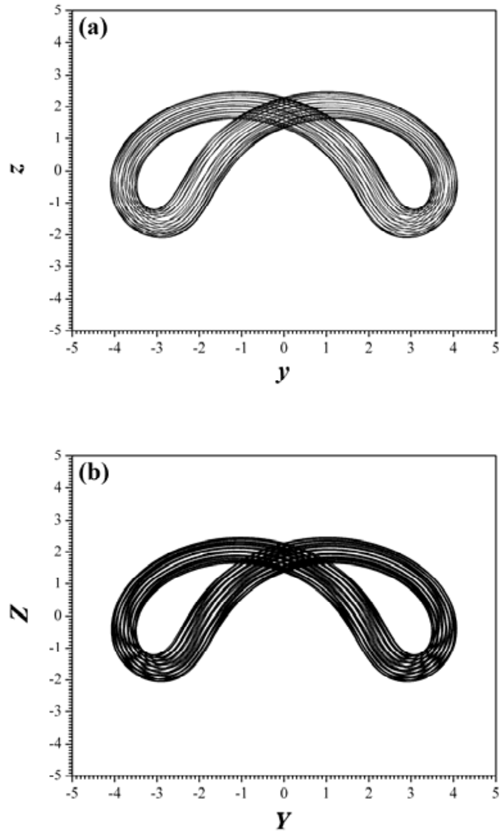

Figure 7. (a) Phase portrait of *z* versus *y* and (b) phase portrait of *Z* versus *Y*, for $a = 2.5$ and $b = 0.83$ (quasiperiodic state).

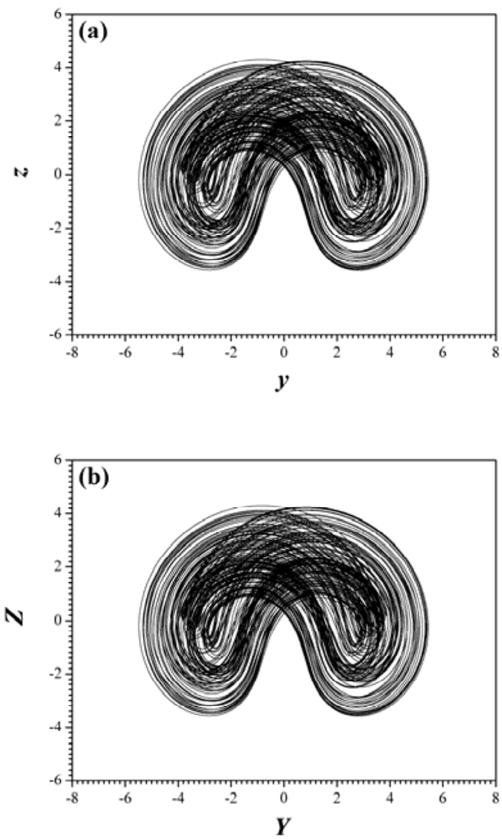

Figure 8. (a) Phase portrait of *z* versus *y* and (b) phase portrait of *Z* versus *Y*, for $a = 2.5$ and $b = 0.55$ (chaotic state).

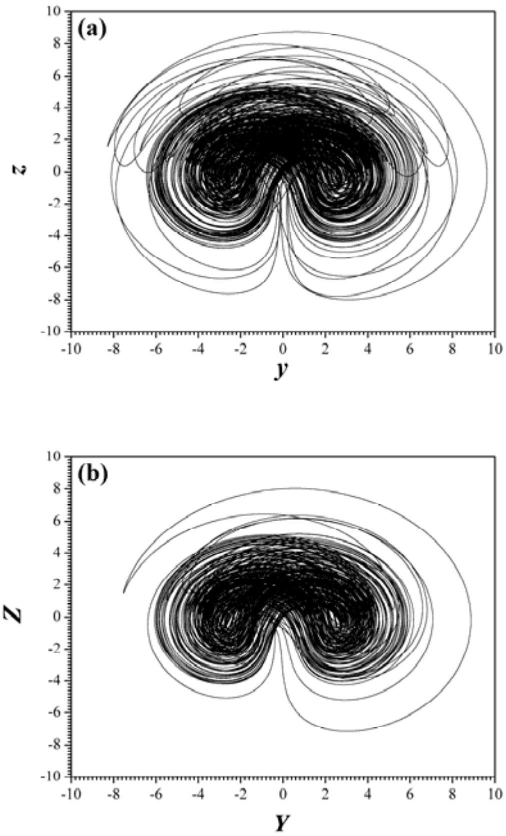

Figure 9. (a) Phase portrait of *z* versus *y* and (b) phase portrait of *Z* versus *Y*, for *a* = 2.5 and *b* = 0.45 (hyperchaotic state).

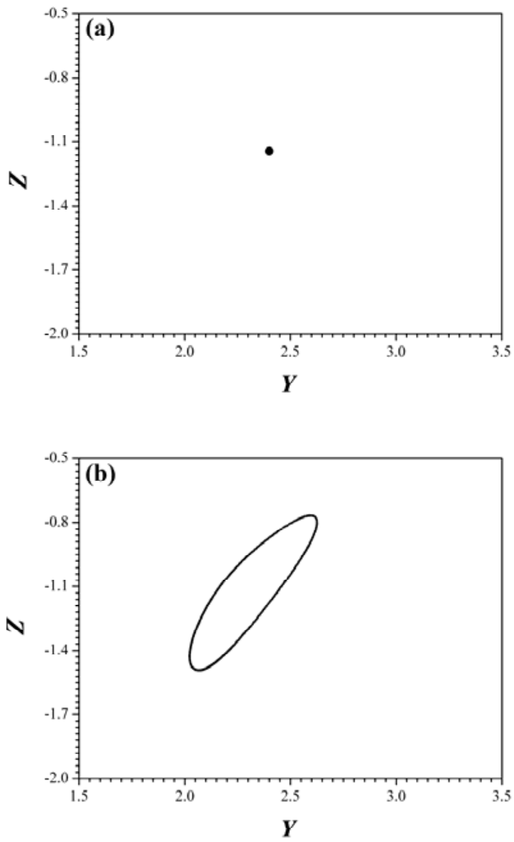

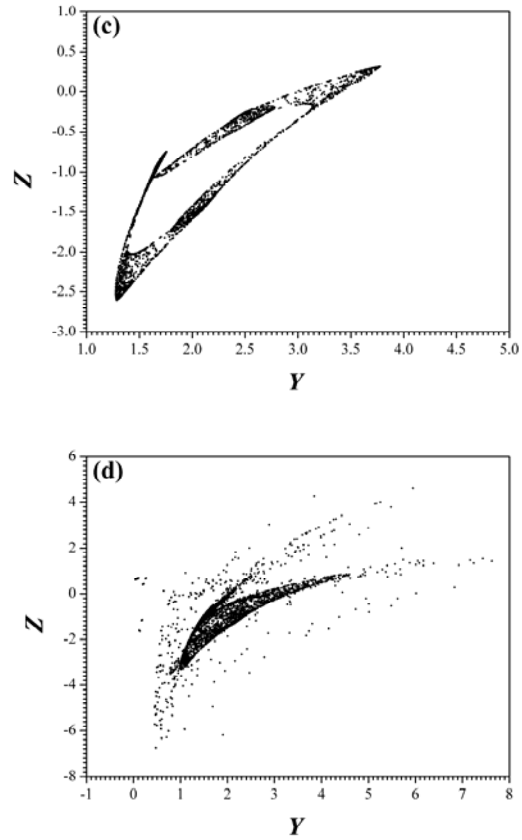

Figure 10. Poincaré maps of *Z* versus *Y*, for (a) *b* = 0.9, (b) *b* = 0.8, (c) *b* = 0.55 and (d) *b* = 0.45, produced using the microcontroller.

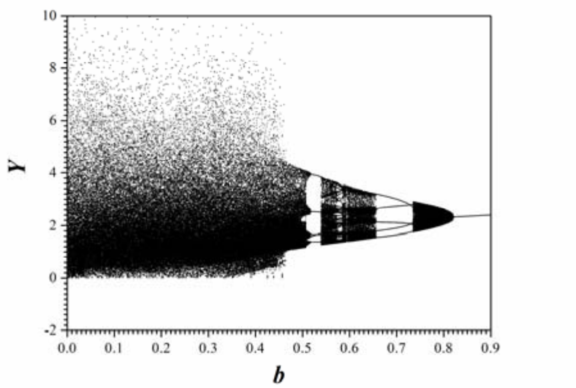

Figure 11. Bifurcation diagram of *Y* versus *b*, for *a* = 2.5, produced using the microcontroller.

4 Conclusion

In this work, a microcontroller was used in order to realize a hyperchaotic oscillator, which belongs to the recently new proposed category of dynamical systems with hidden attractors. By programming the microcontroller, the three most useful tools of nonlinear theory, the phase portrait, the Poincaré map and the bifurcation diagram was produced. The comparison of these with the respective simulation results, which were produced by solving the continuous dynamical system with Runge-Kutta, verified the feasibility of the proposed method. As a future work, the modifications of the algorithms so as to add or substitute the hyperchaotic system will be examined.

References

1. L.D. Kiel and E.W. Elliott, *Chaos theory in the social sciences: Foundations and applications* (Michigan University Press, 1997)
2. S. Banerjee, *Applications of chaos and nonlinear dynamics in engineering* **1**, (Springer, 2011)
3. C. Grebogi, J. Yorke, *The impact of chaos on science and society* (United Nations University Press, 1997)
4. T. Yang, Int. J. Comput. Cogn. **2**, 81-130 (2004)
5. L. Kocarev, IEEE Circ. Syst. Mag. **1**, 6-21 (2001)
6. T. Bräunl, *Embedded robotics: mobile robot design and applications with embedded systems* (Springer Science & Business Media, 2008)
7. W. Wolf, B. Ozer, T. Lv, Computer **35**, 48-53 (2002)
8. R. Alur, K.E. Arzen, J. Baillieul, T.A. Henzinger, *Handbook of networked and embedded control systems* (Springer Science & Business Media, 2007)
9. P. Marwedel, *Embedded system design: Embedded systems foundations of cyber-physical systems* (Springer Science & Business Media, 2010)
10. T. Choudhury, G. Borriello, S. Consolvo, D. Haehnel, B. Harrison, B. Hemingway, L. LeGrand, IEEE Pervasive Computing, **7**, 32-41 (2008)
11. D. Estrin, R. Govindan, J. Heidemann, S. Kumar, *Next century challenges: Scalable coordination in sensor networks*, In: Proceedings of the 5th Annual ACM/IEEE International Conference on Mobile Computing and Networking, 263-270 (1999)
12. R. Bastide, D. Navarre, P. Palanque, A. Schyn, P. Dragicevic, *A model-based approach for real-time embedded multimodal systems in military aircrafts*, In: Proceedings of the 6th International Conference on Multimodal Interfaces, 243-250 (2004)
13. D. Stepner, N. Rajan, D. Hui, *Embedded application design using a real-time OS*, In: 36th IEEE Design Automation Conference, 151-156 (1999)
14. M. Wolf, Newnes (2014)
15. A. Mifdaoui, F. Frances, C. Fraboul, IEEE Trans. Ind. Inform. **6**, 534-547 (2010)
16. C. Cepisca, N.G. Bardis, *Measurement and control in street lighting* (ELECTRA publication 2011)
17. M. Bogdan, M. Buga, R. Medianu, C. Cepisca, N. Bardis, Scientific Bulletin of the Electrical Engineering Faculty, **2**, (2011)
18. C. Cepisca, S.D. Grigorescu, S. Ganatsios, N.G. Bardis, Metrologie **4**, 5-10 (2008)
19. A.K. Aboul-Seoud, E.A. El-Badawy, A. Mokhtar, W. El-Marsy, M. El-Barbry, A.E.D.S. Hafez, *A simple 8 bit digital microcontroller implementation for chaotic sequence generation*, In: Proceedings of the 28th National Radio Science Conference, National Telecomunication Institute, 1-9 (2011)
20. J.D. Serna, A. Joshi, Phys. Educ. **47**, 1-6 (2012)
21. M. Stanciu, O. Datcu, *Atmel AVR microcontroller implementation of a new enciphering algorithm based on a chaotic Generalized Hénon Map*, In: 9th International Conference on Communications, 319-322 (2012)
22. C.K. Volos, I.M. Kyprianidis, I.N. Stouboulos, Robot. Auton. Syst. **61**, 1314-1322 (2013)
23. R. Chiu, M. Mora-Gonzalez, D. Lopez-Mancilla, IERI Procedia **4,** 247-252 (2013)
24. C.K. Volos, J. Comput. Model. **3**, 115-136 (2013)
25. P. Ketthong, W. San-Um, *A robust signum-based piecewise-linaer chaotic map and its application to microcontroller-based cost effective random-bit generator*, In: Proceedings of the International Electrical Engineering Congress 2014, 1-4 (2014)
26. W. San-Um, P. Ketthong, *The generalization of mathematically simple and robust chaotic maps with absolute value nonlinearity*, In IEEE Region Conference TENCON 2014, 1-4 (2014)
27. A.S. Andreatos, C.K. Volos, *Secure text encryption based on hardware chaotic noise generator*, In: 2nd International Conference on Cryptography and Its Applications in the Armed Forces (2014)
28. M. Zapateiro De la Hoz, L. Acho, Y. Vidal, Scientif. World J. **2015** (2015)
29. V.O. Bragin, V.I. Vagaitsev, N.V. Kuznetsov, G.A. Leonov, J. Comput. Syst. Sci. Int. **50**, 511-543 (2011)
30. G.A. Leonov, N.V. Kuznetsov, Int. J. Bifurcat. Chaos **23** 1330002 (2013)
31. T. Kapitaniak, G.A. Leonov, Eur. Phys. J. Special Topics **224**, 1405-1408 (2005)
32. D. Dudkowski, S. Jafari, T. Kapitaniak, N. Kuznetsov, G. Leonov, A. Prasad, Phys. Rep. doi: 10.1016/j.physrep.2016.05.002 (2016)
33. G.A. Leonov, N.V. Kuznetsov, V.I. Vagaitsev, Phys. D **241**, 1482-1486 (2012)
34. S. Brezetskyi, D. Dudkowski, T. Kapitaniak, Eur. Phys. J. Special Topics **224**, 1459-1467 (2015)
35. G.A. Leonov, N.V. Kuznetsov, M.A. Kiseleva, E.P. Solovyeva, A.M. Zaretskiy, Nonlinear Dyn. **77**, 277-288 (2014)
36. G.A. Leonov, N.V. Kuznetsov, T.N. Mokaev, Eur. Phys. J. Special Topics **224**, 142101458 (2015)
37. Z.T. Zhusubaliyev, E. Mosekilde, Comput. Simulat. **109**, 32045 (2015)
38. Z. Gao, C. Zhang, J. Jishou Univ. (Natural Science Edition) **32**, 65-68 (2011)
39. G. Van der Schrier, L.R.M. Maas, Phys. Nonlin. Phenom. **141**, 19-36 (2000)
40. B. Munmuangsaen, B. Srisuchinwong, Phys. Lett. A **373**, 4038-4043 (2009)
41. V. Paar, N. Pavin, Phys. Rev. E **57**, 1544-1549 (1998)
42. A. Wolf, J.B. Swift, J.A. Vastano, Physica D **16**, 285-317 (1985)
43. J.C. Butcher, *Numerical Methods for Ordinary Differential Equations* (John Wiley & Sons 2003)